

1    A content-sensitive framework for modeling episodic  
2    memory reveals event-like structure in naturalistic  
3    experience, recall, and neural processing

4    Andrew C. Heusser, Paxton C. Fitzpatrick, and Jeremy R. Manning

Department of Psychological and Brain Sciences

Dartmouth College, Hanover, NH 03755, USA

Corresponding author: jeremy.r.manning@dartmouth.edu

5    August 29, 2019

6    **Abstract**

7    Our life experiences unfold over time in highly complex manner, with the evolving presence  
8    of numerous intricate features describing our journey between each event we encounter. Here,  
9    we propose a framework for mapping dynamic naturalistic episodes onto geometric spaces as  
10   *experience trajectories* that capture the temporal dynamics of real-world content. Within this  
11   geometric framework, one may compare the shape of the trajectory formed by an experience to  
12   that defined by one's later recollection to characterize our memories' recovery and distortion of  
13   the external world. Here, we apply this approach to a naturalistic memory experiment in which  
14   participants viewed and verbally recounted a video, and find that the video and subsequent  
15   recalls share both an experience-specific shape and a discernible event-like structure. Despite  
16   this apparent similarity, we find that the level of *precision* with which individuals recounted  
17   various events and the *distinctiveness* of recall for those events were varied and predictive of  
18   overall memory performance. Finally, we identify a network of brain structures that is sensitive  
19   to the "shapes" of our ongoing experiences, and an overlapping network sensitive to how we will

20 later remember them. Our framework and findings underscore the rich event-like structure of  
21 the external world and our memories, and offer novel, content-sensitive measures for assessing  
22 episodic memory

23 **Introduction**

24 What does it mean to *remember* something? In traditional episodic memory experiments (e.g.,  
25 list-learning or trial-based experiments; Murdock, 1962; Kahana, 1996), remembering is often cast  
26 as a discrete and binary operation: each studied item may be separated from all others, and la-  
beled as having been recalled or forgotten. More nuanced studies might incorporate self-reported  
27 confidence measures as a proxy for memory strength, or ask participants to discriminate between  
28 “recollecting” the (contextual) details of an experience or having a general feeling of “familiarity”  
29 (Yonelinas, 2002). Using well-controlled, trial-based experimental designs, the field has amassed  
30 a wealth of valuable information regarding human episodic memory. However, there are funda-  
31 mental properties of the external world and our memories that trial-based experiments are not well  
32 suited to capture (for review also see Koriat and Goldsmith, 1994; Huk et al., 2018). First, our expe-  
33 riences and memories are continuous, rather than discrete—removing a (naturalistic) event from  
34 the context in which it occurs can substantially change its meaning. Second, the specific language  
35 used to describe an experience has little bearing on whether the experience should be considered to  
36 have been “remembered.” Asking whether the rememberer has precisely reproduced a specific set  
37 of words to describe a given experience is nearly orthogonal to whether they were actually able to  
38 remember it. In classic (e.g., list-learning) memory studies, by contrast, the number or proportion  
39 of precise recalls is often a primary metric for assessing the quality of participants’ memories.  
40 Third, one might remember the *essence* (or a general summary) of an experience but forget (or  
41 neglect to recount) particular details. Capturing the essence of what happened is typically the  
42 main “point” of recounting a memory to a listener, while the addition of highly specific details  
43 may add comparatively little to successful conveyance of an experience.

45 How might one go about formally characterizing the “essence” of an experience, or whether

46 it has been recovered by the rememberer? Any given moment of an experience derives meaning  
47 from surrounding moments, as well as from longer-range temporal associations (Lerner et al.,  
48 2011; Manning, 2019). Therefore, the timecourse describing how an event unfolds is fundamental  
49 to its overall meaning. Further, this hierarchy formed by our subjective experiences at different  
50 timescales defines a *context* for each new moment (e.g., Howard and Kahana, 2002; Howard et al.,  
51 2014), and plays an important role in how we interpret that moment and remember it later (for  
52 review see Manning et al., 2015). Our memory systems can leverage these associations to form  
53 predictions that help guide our behaviors (Ranganath and Ritchey, 2012). For example, as we  
54 navigate the world, the features of our subjective experiences tend to change gradually (e.g., the  
55 room or situation we are in at any given moment is strongly temporally autocorrelated), allowing  
56 us to form stable estimates of our current situation and behave accordingly (Zacks et al., 2007;  
57 Zwaan and Radvansky, 1998).

58 Although our experiences most often change gradually, they also occasionally change sud-  
59 denly (e.g., when we walk through a doorway; Radvansky and Zacks, 2017). Prior research  
60 suggests that these sharp transitions (termed *event boundaries*) during an experience help to dis-  
61 cretize our experiences (and their mental representations) into *events* (Radvansky and Zacks, 2017;  
62 Brunec et al., 2018; Heusser et al., 2018a; Clewett and Davachi, 2017; Ezzyat and Davachi, 2011;  
63 DuBrow and Davachi, 2013). The interplay between the stable (within event) and transient (across  
64 event) temporal dynamics of an experience also provides a potential framework for transforming  
65 experiences into memories that distill those experiences down to their essence. For example, prior  
66 work has shown that event boundaries can influence how we learn sequences of items (Heusser  
67 et al., 2018a; DuBrow and Davachi, 2013), navigate (Brunec et al., 2018), and remember and un-  
68 derstand narratives (Zwaan and Radvansky, 1998; Ezzyat and Davachi, 2011). Prior research has  
69 implicated the hippocampus and the medial prefrontal cortex as playing a critical role in trans-  
70 forming experiences into structured and consolidated memories (Tompry and Davachi, 2017).

71 Here we sought to examine how the temporal dynamics of a “naturalistic” experience were  
72 later reflected in participants’ memories. We analyzed an open dataset that comprised behavioral  
73 and functional Magnetic Resonance Imaging (fMRI) data collected as participants viewed and then

74 verbally recounted an episode of the BBC television series *Sherlock* (Chen et al., 2017). We developed  
75 a computational framework for characterizing the temporal dynamics of the moment-by-moment  
76 content of the episode and of participants' verbal recalls. Specifically, we use topic modeling (Blei  
77 et al., 2003) to characterize the thematic conceptual (semantic) content present in each moment of  
78 the episode and recalls, and Hidden Markov Models (Rabiner, 1989; Baldassano et al., 2017) to  
79 discretize this evolving semantic content into events. In this way, we cast naturalistic experiences  
80 (and recalls of those experiences) as *trajectories* that describe how the experiences evolve over  
81 time. Under this framework, successful remembering entails verbally "traversing" the content  
82 trajectory of the episode, thereby reproducing the shape (or essence) of the original experience.  
83 Comparing the shapes of the topic trajectories of the episode and of participants' retellings of the  
84 episode then reveals which aspects of the episode were preserved (or lost) in the translation into  
85 memory. We further examine whether 1) the *precision* with which a participant recounts each event  
86 and 2) the *distinctiveness* each recall event is (relative to the other recalled events) relates to their  
87 overall memory performance. Last, we identify networks of brain structures whose responses  
88 (as participants watched the episode) reflected the temporal dynamics of the episode, and how  
89 participants would later recount the episode.

## 90 Results

91 To characterize the shape of the *Sherlock* episode and participants' subsequent recounts of its  
92 unfolding, we used a topic model (Blei et al., 2003) to discover the latent themes in the episode's  
93 dynamic content. Topic models take as inputs a vocabulary of words to consider and a collection  
94 of text documents, and return two output matrices. The first of these is a *topics matrix* whose rows  
95 are topics (latent themes) and whose columns correspond to words in the vocabulary. The entries  
96 of the topics matrix define how each word in the vocabulary is weighted by each discovered topic.  
97 For example, a detective-themed topic might weight heavily on words like "crime," and "search."  
98 The second output is a *topic proportions matrix*, with one row per document and one column per  
99 topic. The topic proportions matrix describes what mixture of discovered topics is reflected in each

100 document.

101 Chen et al. (2017) collected hand-annotated information about each of 1000 (manually identified)  
102 scenes spanning the roughly 50 minute video used in their experiment. This information included:  
103 a brief narrative description of what was happening; whether the scene took place indoors or  
104 outdoors; the names of any characters on the screen; the names of any characters who were in  
105 focus in the camera shot; the names of characters who were speaking; the location where the scene  
106 took place; the camera angle (close up, medium, long, etc.); whether or not background music was  
107 present; and other similar details (for a full list of annotated features see *Methods*). We took from  
108 these annotations the union of all unique words (excluding stop words, such as “and,” “or,” “but,”  
109 etc.) across all features and scenes as the “vocabulary” for the topic model. We then concatenated  
110 the sets of words across all features contained in overlapping, 50-scene sliding windows, and  
111 treated each 50-scene sequence as a single “document” for the purpose of fitting the topic model.  
112 Next, we fit a topic model with (up to)  $K = 100$  topics to this collection of documents. We found that  
113 27 unique topics (with non-zero weights) were sufficient to describe the time-varying content of the  
114 video (see *Methods*; Figs. 1, S2). Note that our approach is similar in some respects to Dynamic Topic  
115 Models (Blei and Lafferty, 2006) in that we sought to characterize how the thematic content of the  
116 episode evolved over time. However, whereas Dynamic Topic Models are designed to characterize  
117 how the properties of *collections* of documents change over time, our sliding window approach  
118 allows us to examine the topic dynamics within a single document (or video). Specifically, our  
119 approach yielded (via the topic proportions matrix) a single *topic vector* for each timepoint of the  
120 episode (we set timepoints to match the acquisition times of the 1976 fMRI volumes collected as  
121 participants viewed the episode).

122 The topics we found were heavily character-focused (e.g., the top-weighted word in each topic  
123 was nearly always a character) and could be roughly divided into themes that were primarily  
124 Sherlock Holmes-focused (Sherlock is the titular character), primarily John Watson-focused (John  
125 is Sherlock’s close confidant and assistant), or focused on Sherlock and John interacting (Fig. S2).  
126 Several of the topics were highly similar, which we hypothesized might allow us to distinguish  
127 between subtle narrative differences (if the distinctions between those overlapping topics were



**Figure 1: Methods overview.** We used hand-annotated descriptions of each moment of video to fit a topic model. Three example video frames and their associated descriptions are displayed (top two rows). Participants later recalled the video (in the third row, we show example recalls of the same three scenes from participant 13). We used the topic model (fit to the annotations) to estimate topic vectors for each moment of video and each sentence the participants recalled. Example topic vectors are displayed in the bottom row (blue: video annotations; green: example participant’s recalls). Three topic dimensions are shown (the highest-weighted topics for each of the three example scenes, respectively). We also show the ten highest-weighted words for each topic. Figure S2 provides a full list of the top 10 words from each of the discovered topics.

128 meaningful; also see Fig. S3). The topic vectors for each timepoint were *sparse*, in that only a small  
129 number (usually one or two) of topics tended to be “active” in any given timepoint (Fig. 2A).  
130 Further, the dynamics of the topic activations appeared to exhibit *persistance* (i.e., given that a  
131 topic was active in one timepoint, it was likely to be active in the following timepoint) along with  
132 *occasional rapid changes* (i.e., occasionally topics would appear to spring into or out of existence).  
133 These two properties of the topic dynamics may be seen in the block diagonal structure of the  
134 timepoint-by-timepoint correlation matrix (Fig. 2B) and reflect the gradual drift and sudden shifts  
135 fundamental to the contextual dynamics of real-world experiences. Given this observation, we  
136 adapted an approach devised by Baldassano et al. (2017), and used a Hidden Markov Model (HMM)  
137 to identify the *event boundaries* where the topic activations changed rapidly (i.e., at the boundaries  
138 of the blocks in the correlation matrix; event boundaries identified by the HMM are outlined in  
139 yellow). Part of our model fitting procedure required selecting an appropriate number of “events”  
140 to segment the timeseries into. We used an optimization procedure to identify the number of  
141 events that maximized within-event stability while also minimizing across-event correlations (see  
142 *Methods* for additional details). To create a stable “summary” of the video, we computed the  
143 average topic vector within each event (Fig. 2C).

144 Given that the time-varying content of the video could be segmented cleanly into discrete  
145 events, we wondered whether participants’ recalls of the video also displayed a similar structure.  
146 We applied the same topic model (already trained on the video annotations) to each participant’s  
147 recalls. Analogous to how we analyzed the time-varying content of the video, to obtain similar  
148 estimates for participants’ recalls, we treated each (overlapping) 10-sentence “window” of their  
149 transcript as a “document” and then computed the most probable mix of topics reflected in each  
150 timepoint’s sentences. This yielded, for each participant, a number-of-sentences by number-of-  
151 topics topic proportions matrix that characterized how the topics identified in the original video  
152 were reflected in the participant’s recalls. Note that an important feature of our approach is  
153 that it allows us to compare participant’s recalls to events from the original video, despite that  
154 different participants may have used different language to describe the same event, and that those  
155 descriptions may not match the original annotations. This is a substantial benefit of projecting

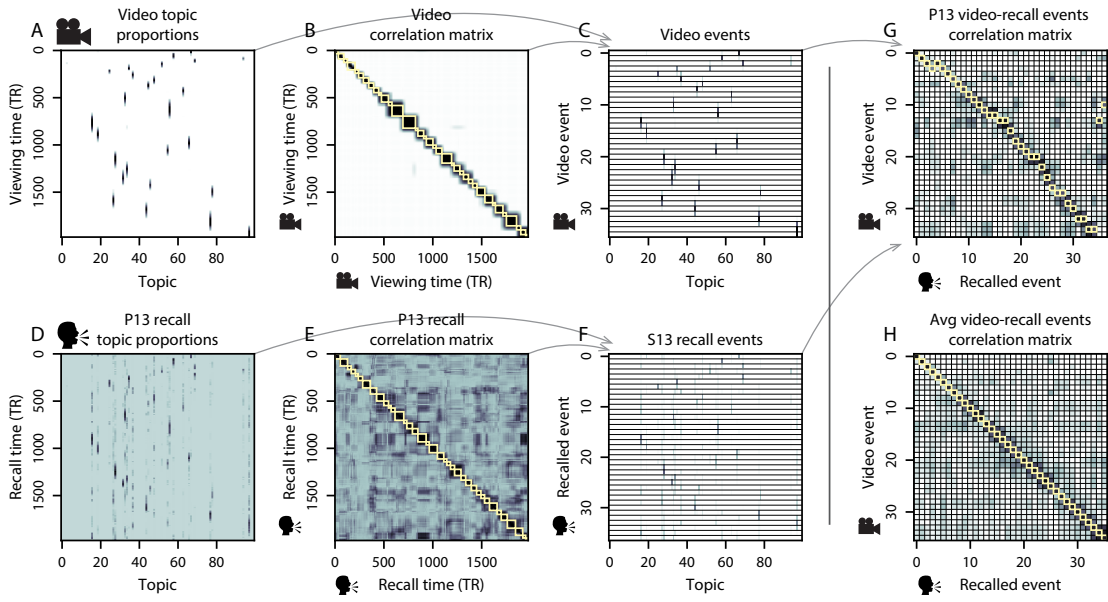


**Figure 2: Modelling naturalistic stimuli and recalls.** All panels: darker colors indicate greater values; range: [0, 1]. **A.** Topic vectors ( $K = 100$ ) for each of the 1976 video timepoints. **B.** Timepoint-by-timepoint correlation matrix of the topic vectors displayed in Panel A. Event boundaries detected by the HMM are denoted in yellow (36 events detected). **C.** Average topic vectors for each of the 36 video events. **D.** Topic vectors for each of 294 sentences spoken by an example participant while recalling the video, resampled to match the timeseries of the video. **E.** Timepoint-by-timepoint correlation matrix of the topic vectors displayed in Panel D. Event boundaries detected by the HMM are denoted in yellow (37 events detected). **F.** Average topic vectors for each of the 37 recalled events from the example participant. **G.** Correlations between the topic vectors for every pair of video events (Panel C) and recalled events (from the example participant; Panel F). For similar plots for all participants see Figure S5. **H.** Average correlations between each pair of video events and recalled events (across all 17 participants). To create the figure, each recalled event was assigned to the video event with the most correlated topic vector (yellow boxes in panels G and H). The heat maps in each panel were created using Seaborn (Waskom et al., 2016).

156 the video and recalls into a shared “topic” space. An example topic proportions matrix from one  
157 participant’s recalls is shown in Figure 2D.

158 Although the example participant’s recall topic proportions matrix has some visual similarity to  
159 the video topic proportions matrix, the time-varying topic proportions for the example participant’s  
160 recalls are not as sparse as for the video (e.g., compare Figs. 2A and D). Similarly, although there  
161 do appear to be periods of stability in the recall topic dynamics (e.g., most topics are active or  
162 inactive over contiguous blocks of time), the overall timecourses are not as cleanly delineated as  
163 the video topics are. To examine these patterns in detail, we computed the timepoint-by-timepoint  
164 correlation matrix for the example participant’s recall topic proportions (Fig. 2E). As in the video  
165 correlation matrix (Fig. 2B), the example participant’s recall correlation matrix has a strong block  
166 diagonal structure, indicating that their recalls are discretized into separated events. As for the  
167 video correlation matrix, we can use an HMM, along with the aforementioned number-of-events  
168 optimization procedure (also see *Methods*) to determine how many events are reflected in the  
169 participant’s recalls and where specifically the event boundaries fall (outlined in yellow). We  
170 carried out a similar analysis on all 17 participants’ recall topic proportions matrices (Fig. S4).

171 Two clear patterns emerged from this set of analyses. First, although every individual partic-  
172 ipant’s recalls could be segmented into discrete events (i.e., every individual participant’s recall  
173 correlation matrix exhibited clear block diagonal structure; Fig. S4), each participant appeared to  
174 have a unique *recall resolution*, reflected in the sizes of those blocks. For example, some participants’  
175 recall topic proportions segmented into just a few events (e.g., Participants P2, P6, and P14), while  
176 others’ recalls segmented into many shorter duration events (e.g., Participants P12, P13, and P17).  
177 This suggests that different participants may be recalling the video with different levels of detail-  
178 e.g., some might touch on just the major plot points, whereas others might attempt to recall every  
179 minor scene or action. The second clear pattern present in every individual participant’s recall  
180 correlation matrix is that, unlike in the video correlation matrix, there are substantial off-diagonal  
181 correlations. Whereas each event in the original video was (largely) separable from the others  
182 (Fig. 2B), in transforming those separable events into memory, participants appear to be integrat-  
183 ing across multiple events, blending elements of previously recalled and not-yet-recalled events

184 into each newly recalled event (Figs. 2D, S4; also see Manning et al., 2011; Howard et al., 2012).

185 The above results indicate that both the structure of the original video and participants' recalls  
186 of the video exhibit event boundaries that can be identified automatically by characterizing the  
187 dynamic content using a shared topic model and segmenting the content into events using HMMs.  
188 Next, we asked whether some correspondence might be made between the specific content of the  
189 events the participants experienced in the video, and the events they later recalled. One approach  
190 to linking the experienced (video) and recalled events is to label each recalled event as matching  
191 the video event with the most similar (i.e., most highly correlated) topic vector (Figs. 2G, S5). This  
192 yields a sequence of "presented" events from the original video, and a (potentially differently  
193 ordered) sequence of "recalled" events for each participant. Analogous to classic list-learning  
194 studies, we can then examine participants' recall sequences by asking which events they tended  
195 to recall first (probability of first recall; Fig. 3A; Welch and Burnett, 1924; Postman and Phillips,  
196 1965; Atkinson and Shiffrin, 1968); how participants most often transition between recalls of the  
197 events as a function of the temporal distance between them (lag-conditional response probability;  
198 Fig. 3B; Kahana, 1996); and which events they were likely to remember overall (serial position  
199 recall analyses; Fig. 3C; Murdock, 1962). Interestingly, for two of these analyses (probability of first  
200 recall and lag-conditional response probability curves) we observe patterns comparable to classic  
201 effects from the list-learning literature: namely, a higher probability of initiating recall with the  
202 first event in the sequence (Fig. 3A) and a higher probability of transitioning to neighboring events  
203 with an asymmetric forward bias (Fig. 3C). In contrast, we do not observe a pattern comparable to  
204 the serial position effect (Fig. 3C), but rather we see higher memory for specific events distributed  
205 somewhat evenly throughout the video.

206 We can also apply two list-learning-native analyses that describe how participants group items  
207 in their recall sequences: temporal clustering and semantic clustering (Polyn et al., 2009, see  
208 *Methods* for details). Temporal clustering refers to the extent to which participants group their  
209 recall responses according to encoding position. Semantic clustering measures the extent to which  
210 participants cluster their recall responses according to semantic similarity. Overall, we found that  
participants heavily clustered video events in their recalls by both temporal proximity (mean:

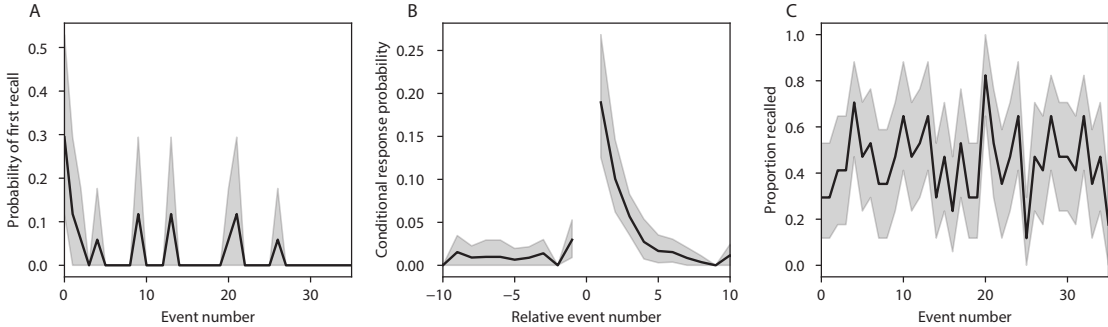


**Figure 3: Naturalistic extensions of classic list-learning memory analyses.** **A.** The probability of first recall as a function of the serial position of the event in the video. **B.** The probability of recalling each event, conditioned on having most recently recalled the event *lag* events away in the video. **C.** The proportion of participants who recalled each event, as a function of the serial position of the events in the video. All panels: error bars denote bootstrap-estimated standard error of the mean.

212 0.860, SEM: 0.016) and semantic content (mean: 0.888, SEM: 0.014).

213 Statistical models of memory studies often treat memory recalls as binary (e.g. the item was re-  
 214 called or not) and independent events. However, our framework produces a content-based model  
 215 of individual stimulus and recall events, allowing for direct quantitative comparison between all  
 216 stimulus and recall events, as well as between the recall events themselves. Leveraging these  
 217 content-based models of the stimulus/recall events, we developed two novel metrics for quanti-  
 218 fying naturalistic memory representations: *precision* and *distinctiveness*. We define precision as the  
 219 average correlation between the topic proportions of each recall event and the maximally corre-  
 220 lated video event (Fig. 4). Participants whose recall events are more veridical descriptions of what  
 221 happened in the video event will presumably have higher precision scores. We find that, across  
 222 participants, a higher precision score is correlated to both hand-annotated memory performance  
 223 (Pearson's  $r(15) = 0.55, p = 0.021$ ) and the number of recall events estimated by our model (Pear-  
 224 son's  $r(15) = 0.66, p = 0.004$ ). A second novel metric we introduce here is distinctiveness, or how  
 225 unique the recall description was to each video event. We define distinctiveness as 1 minus the av-  
 226 erage of all non-matching recall events from the video-recall correlation matrix. We hypothesized  
 227 that participants who recounted events in a more distinctive way would display better overall  
 228 memory. Similarly to precision, we find that the more distinct participants recalls are (on average),

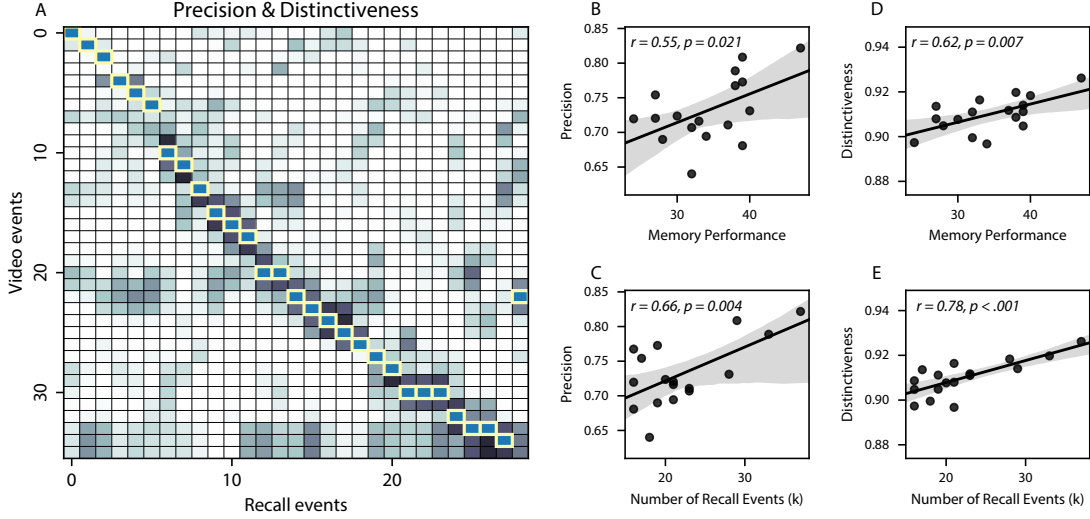


**Figure 4: Novel content-based metrics of naturalistic memory: precision and distinctiveness.** **A.** A video-recall correlation matrix for a representative participant (17). The yellow boxes highlight the maximum correlation in each column. Precision was computed as the average of the maximum correlation in each column. On the other hand, distinctiveness was defined as the average of everything except for the maximum correlation in each column. **B.** The (Pearson's) correlation between precision and hand-annotated memory performance. **C.** The correlation between precision and the number of events recovered by the model ( $k$ ). **D.** The correlation between distinctiveness and hand-annotated memory performance. **E.** The correlation between distinctiveness and the number of events recovered by the model ( $k$ ).

the more they remembered (hand-annotated memory: Pearson's  $r(15) = 0.62, p = 0.007$ ; number of events: Pearson's  $r(15) = 0.78, p < 0.001$ ). In summary, using two novel metrics afforded by our approach, we find that participants whose recalls are both more precise and distinct remember more content.

The prior analyses leverage the correspondence between the 100-dimensional topic proportion matrices for the video and participants' recalls to characterize recall. However, it is difficult to gain deep insights into that content solely by examining the topic proportion matrices (e.g., Figs. 2A, D) or the corresponding correlation matrices (Figs. 2B, E, S4). To visualize the time-varying high-dimensional content in a more intuitive way (Heusser et al., 2018b) we projected the topic proportions matrices onto a two-dimensional space using Uniform Manifold Approximation and Projection (UMAP; McInnes and Healy, 2018). In this lower-dimensional space, each point

240 represents a single video or recall event, and the distances between the points reflect the distances  
241 between the events' associated topic vectors (Fig. 5). In other words, events that are near to each  
242 other in this space are more semantically similar.

243 Visual inspection of the video and recall topic trajectories reveals a striking pattern. First,  
244 the topic trajectory of the video (which reflects its dynamic content; Fig. 5A) is captured nearly  
245 perfectly by the averaged topic trajectories of participants' recalls (Fig. 5B). To assess the consistency  
246 of these recall trajectories across participants, we asked: given that a participant's recall trajectory  
247 had entered a particular location in topic space, could the position of their *next* recalled event  
248 be predicted reliably? For each location in topic space, we computed the set of line segments  
249 connecting successively recalled events (across all participants) that intersected that location (see  
250 *Methods* for additional details). We then computed (for each location) the distribution of angles  
251 formed by the lines defined by those line segments and a fixed reference line (the *x*-axis). Rayleigh  
252 tests revealed the set of locations in topic space at which these across-participant distributions  
253 exhibited reliable peaks (blue arrows in Fig. 5B reflect significant peaks at  $p < 0.05$ , corrected). We  
254 observed that the locations traversed by nearly the entire video trajectory exhibited such peaks.  
255 In other words, participants exhibited similar trajectories that also matched the trajectory of the  
256 original video (Fig. 5C). This is especially notable when considering the fact that the number of  
257 events participants recalled (dots in Fig. 5C) varied considerably across people, and that every  
258 participant used different words to describe what they had remembered happening in the video.  
259 Differences in the numbers of remembered events appear in participants' trajectories as differences  
260 in the sampling resolution along the trajectory. We note that this framework also provides a  
261 means of detangling classic "proportion recalled" measures (i.e., the proportion of video events  
262 referenced in participants' recalls) from participants' abilities to recapitulate the full shape of the  
263 original video (i.e., the similarity in the shape of the original video trajectory and that defined by  
264 each participant's recounting of the video).

265 Because our analysis framework projects the dynamic video content and participants' recalls  
266 onto a shared topic space, and because the dimensions of that space are known (i.e., each topic  
267 dimension is a set of weights over words in the vocabulary; Fig. S2), we can examine the topic

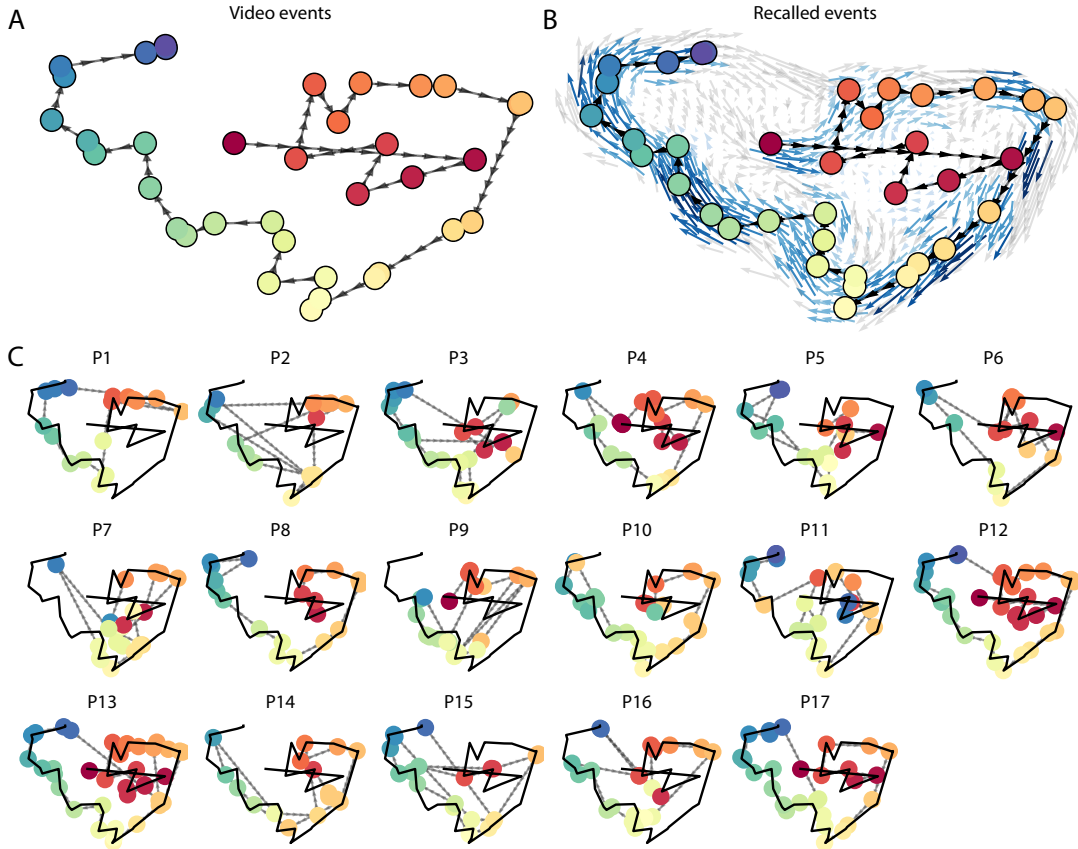


**Figure 5: Trajectories through topic space capture the dynamic content of the video and recalls.** All panels: the topic proportion matrices have been projected onto a shared two-dimensional space using UMAP. **A.** The two-dimensional topic trajectory taken by the episode of *Sherlock*. Each dot indicates an event identified using the HMM (see *Methods*); the dot colors denote the order of the events (early events are in red; later events are in blue), and the connecting lines indicate the transitions between successive events. **B.** The average two-dimensional trajectory captured by participants' recall sequences, with the same format and coloring as the trajectory in Panel A. To compute the event positions, we matched each recalled event with an event from the original video (see *Results*), and then we averaged the positions of all events with the same label. The arrows reflect the average transition direction through topic space taken by any participants whose trajectories crossed that part of topic space; blue denotes reliable agreement across participants via a Rayleigh test ( $p < 0.05$ , corrected). **C.** The recall topic trajectories (gray) taken by each individual participant (P1–P17). The video's trajectory is shown in black for reference. (Same format and coloring as Panel A.)

268 trajectories to understand which specific content was remembered well (or poorly). For each video  
269 event, we can ask: what was the average correlation (across participants) between the video event's  
270 topic vector and the closest matching recall event topic vectors from each participant? This yields a  
271 single correlation coefficient for each video event, describing how closely participants' recalls of the  
272 event tended to reliably capture its content (Fig. 6A). (We also examined how different comparisons  
273 between each video event's topic vector and the corresponding recall event topic vectors related  
274 to hand-annotated characterizations of memory performance; see *Supporting Information*). Given  
275 this summary of which events were recalled reliably (or not), we next asked whether the better-  
276 remembered or worse-remembered events tended to reflect particular topics. We computed a  
277 weighted average of the topic vectors for each video event, where the weights reflected how reliably  
278 each event was recalled. To visualize the result, we created a "wordle" image (Mueller et al., 2018)  
279 where words weighted more heavily by better-remembered topics appear in a larger font (Fig. 6B,  
280 green box). Events that reflected topics weighting heavily on characters like "Sherlock" and "John"  
281 (i.e., the main characters) and locations like "221b Baker Street" (i.e., a major recurring location and  
282 the address of the flat that Sherlock and John share) were best remembered. An analogous analysis  
283 revealed which themes were poorly remembered. Here in computing the weighted average over  
284 events' topic vectors, we weighted each event in *inverse* proportion to how well it was remembered  
285 (Fig. 6B, red box). This revealed that events with relatively minor characters such as "Mike,"  
286 "Jeffrey," and "Molly," as well as less-integral plot locations (e.g., "hospital" and "office") were  
287 least well-remembered. This suggests that what is retained in memory are the major plot elements  
288 (i.e., the overall shape of what happened), whereas the more minor details are prone to pruning.

289 In addition to constructing overall summaries, assessing the video and recall topic vectors  
290 from individual events can provide further insights. Specifically, for any given event we can  
291 construct two wordles: one from the original video event's topic vector, and a second from the  
292 average topic vectors produced by all participants' recalls of that event. We can then examine those  
293 wordles visually to gain an intuition for which aspects of the video event were recapitulated in  
294 participants' recalls. Several example wordles are displayed in Figure 6C (wordles from the three  
295 best-remembered events are circled in green; wordles from the three worst-remembered events

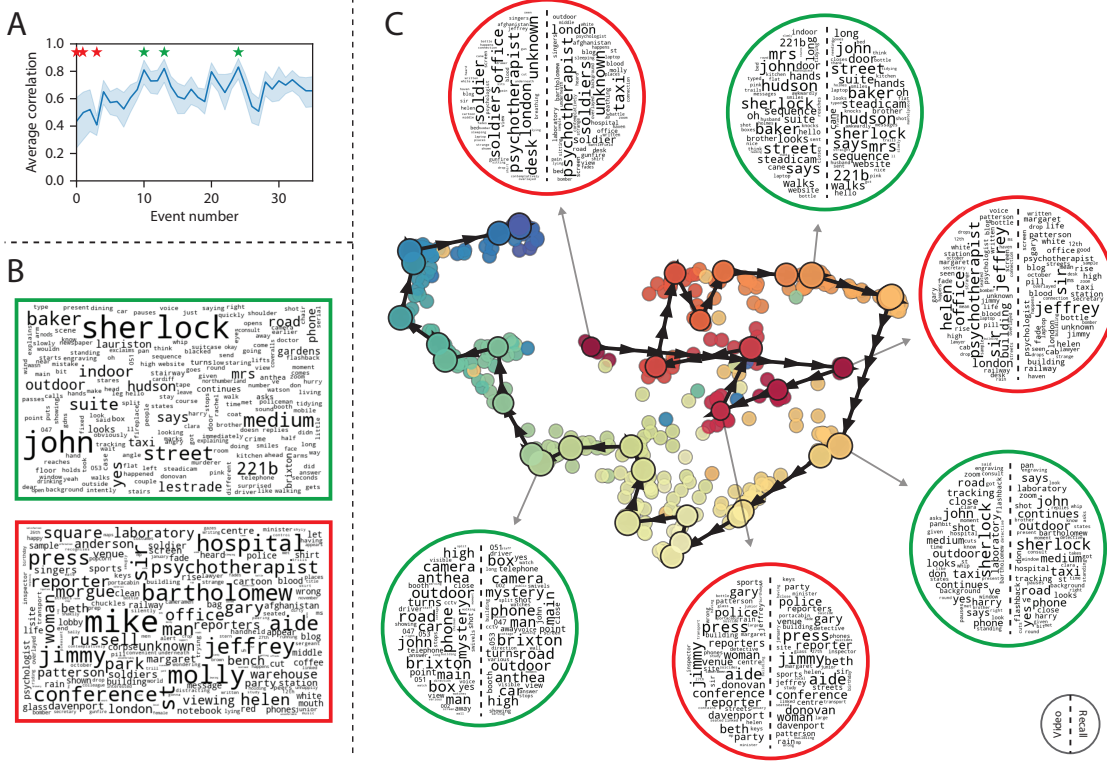


**Figure 6: Transforming experience into memory.** **A.** Average correlations (across participants) between the topic vectors from each video event and the closest-matching recall events. Error bars denote bootstrap-derived across-participant 95% confidence intervals. The stars denote the three best-remembered events (green) and worst-remembered events (red). **B.** Wordles comprising the top 200 highest-weighted words reflected in the weighted-average topic vector across video events. Green: video events were weighted by how well the topic vectors derived from recalls of those events matched the video events' topic vectors (Panel A). Red: video events were weighted by the inverse of how well their topic vectors matched the recalled topic vectors. **C.** The set of all video and recall events is projected onto the two-dimensional space derived in Figure 5. The dots outlined in black denote video events (dot size reflects the average correlation between the video event's topic vector and the topic vectors from the closest matching recalled events from each participant; bigger dots denote stronger correlations). The dots without black outlines denote recalled events. All dots are colored using the same scheme as Figure 5A. Wordles for several example events are displayed (green: three best-remembered events; red: three worst-remembered events). Within each circular wordle, the left side displays words associated with the topic vector for the video event, and the right side displays words associated with the (average) recall event topic vector, across all recall events matched to the given video event.

296 are circled in red). Using wordles to visually compare the topical content of each video event and  
297 the (average) corresponding recall event reveals the specific content from the specific events that  
298 is reliably retained in the transformation into memory (green events) or not (red events).

299 The results thus far inform us about which aspects of the dynamic content in the episode  
300 participants watched were preserved or altered in participants' memories of the episode. We next  
301 carried out a series of analyses aimed at understanding which brain structures might implement  
302 these processes. In one analysis we sought to identify which brain structures were sensitive  
303 to the video's dynamic content, as characterized by its topic trajectory. Specifically, we used a  
304 searchlight procedure to identify the extent to which each cluster of voxels exhibited a timecourse  
305 of activity (as the participants watched the video) whose temporal correlation matrix matched  
306 the temporal correlation matrix of the original video's topic proportions (Fig. 2B). As shown  
307 in Figure 7A, the analysis revealed a network of regions including bilateral frontal cortex and  
308 cingulate cortex, suggesting that these regions may play a role in processing information relevant  
309 to the narrative structure of the video. In a second analysis, we sought to identify which brain  
310 structures' responses (while viewing the video) reflected how each participant would later *recall*  
311 the video. We used an analogous searchlight procedure to identify clusters of voxels whose  
312 temporal correlation matrices reflected the temporal correlation matrix of the topic proportions for  
313 each individual's recalls (Figs. 2D, S4). As shown in Figure 7B, the analysis revealed a network of  
314 regions including the ventromedial prefrontal cortex (vmPFC), anterior cingulate cortex (ACC), and  
315 right medial temporal lobe (rMTL), suggesting that these regions may play a role in transforming  
316 each individual's experience into memory. In identifying regions whose responses to ongoing  
317 experiences reflect how those experiences will be remembered later, this latter analysis extends  
318 classic *subsequent memory analyses* (e.g., Paller and Wagner, 2002) to domain of naturalistic stimuli.

## 319 Discussion

320 Our work casts remembering as reproducing (behaviorally and neurally) the topic trajectory, or  
321 shape, of an experience. This view draws inspiration from prior work aimed at elucidating

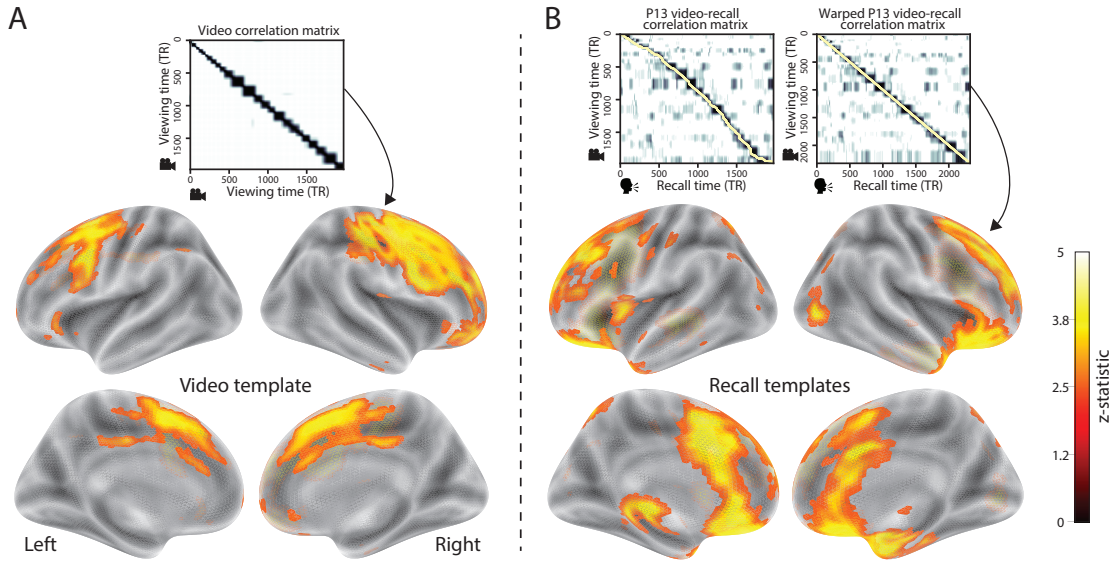


**Figure 7: Brain structures that underlie the transformation of experience into memory.** **A.** We searched for regions whose responses (as participants watched the video) matched the temporal correlation matrix of the video topic proportions. These regions are sensitive to the narrative structure of the video. **B.** We searched for regions whose responses (as participants watched the video) matched the temporal correlation matrix of the topic proportions derived from each individual's later recall of video. These regions are sensitive to how the narrative structure of the video is transformed into a memory of the video. Both panels: the maps are thresholded at  $p < 0.05$ , corrected.

the neural and behavioral underpinnings of how we process dynamic naturalistic experiences and remember them later. One approach to identifying neural responses to naturalistic stimuli (including experiences) entails building a model of the stimulus and searching for brain regions whose responses are consistent with the model. In prior work, a series of studies from Uri Hasson’s group (Lerner et al., 2011; Simony et al., 2016; Chen et al., 2017; Baldassano et al., 2017; Zadbood et al., 2017) have extended this approach with a clever twist: rather than building an explicit stimulus model, these studies instead search for brain responses (while experiencing the stimulus) that are reliably similar across individuals. So called *inter-subject correlation* (ISC) and *inter-subject functional connectivity* (ISFC) analyses effectively treat other people’s brain responses to the stimulus as a “model” of how its features change over time. By contrast, in our present work we used topic models and HMMs to construct an explicit stimulus model (i.e., the topic trajectory of the video). When we searched for brain structures whose responses are consistent with the video’s topic trajectory, we identified a network of structures that overlapped strongly with the “long temporal receptive window” network reported by the Hasson group (e.g., compare our Fig. 7A with the map of long temporal receptive window voxels in Lerner et al., 2011). This provides support for the notion that part of the long temporal receptive window network may be maintaining an explicit model of the stimulus dynamics. When we performed a similar analysis after swapping out the video’s topic trajectory with the recall topic trajectories of each individual participant, this allowed us to identify brain regions whose responses (as the participants viewed the video) reflected how the video trajectory would be transformed in memory (as reflected by the recall topic trajectories). The analysis revealed that the rMTL and vmPFC may play a role in this person-specific transformation from experience into memory. The role of the MTL in episodic memory encoding has been well-reported (e.g., Paller and Wagner, 2002; Davachi et al., 2003; Ranganath et al., 2004; Davachi, 2006; Wiltgen and Silva, 2007; Diana et al., 2007; van Kesteren et al., 2013). Prior work has also implicated the medial prefrontal cortex in representing “schema” knowledge (i.e., general knowledge about the format of an ongoing experience given prior similar experiences; van Kesteren et al., 2012, 2013; Schlichting and Preston, 2015; Gilboa and Marlatte, 2017; Spalding et al., 2018). Integrating across our study and this prior work, one interpretation is

350 that the person-specific transformations mediated (or represented) by the rMTL and vmPFC may  
351 reflect schema knowledge being leveraged, formed, or updated, incorporating ongoing experience  
352 into previously acquired knowledge.

353 In extending classical free recall analyses to our naturalistic memory framework, we recovered  
354 two patterns of recall dynamics central to list-learning studies: a high probability of initiating  
355 recall with the first video event (Fig. 3A) and a strong bias toward transitioning from recalling a  
356 given event to recalling the event immediately following it (Fig. 3B). However, equally noteworthy  
357 are the typical free recall results not recovered in these analyses, as each highlights a fundamental  
358 difference between list-learning studies and naturalistic memory paradigms like the one employed  
359 in the present study. The most noticeable departure from hallmark free recall dynamics in these  
360 findings is the apparent lack of a serial position effect in Figure 3C, which instead shows greater  
361 and lesser recall probabilities for events distributed across the video stimulus. Stimuli in free recall  
362 experiments most often comprise lists of simple, common words, presented to participants in a  
363 random order. (In fact, numerous word pools have been developed based on these criteria; e.g.,  
364 Friendly et al., 1982). These stimulus qualities enable two assumptions that are central to word  
365 list analyses, but frequently do not hold for real-world experiences. First, researchers conducting  
366 free recall studies may assume that the content at each presentation index is essentially equal, and  
367 does not bear qualities that would cause participants to remember it more or less successfully than  
368 others. Such is rarely the case with real-world experiences or experiments meant to approximate  
369 them, and the effects of both intrinsic and observer-dependent factors on stimulus memorability  
370 are well established (for review see Chun and Turk-Browne, 2007; Bylinskii et al., 2015; Tyng  
371 et al., 2017). Second, the random ordering of list items ensures that (across participants, on  
372 average) there is no relationship between the thematic similarity of individual stimuli and their  
373 presentation positions—in other words, two semantically related words are no more likely to be  
374 presented next to each other than at opposite ends of the list. In most cases, the exact opposite  
375 is true of real-world episodes. Our internal thoughts, our actions, and the physical state of the  
376 world around us all tend to follow a direct, causal progression. As a result, each moment of our  
377 experience tends to be inherently more similar to surrounding moments than to those in the distant

378 past or future. Memory literature has termed this strong temporal autocorrelation “context,” and  
379 in various media that depict real-world events (e.g., movies and written stories), we recognize  
380 it as a *narrative structure*. While a random word list (by definition) has no such structure, the  
381 logical progression between ideas and actions in a naturalistic stimulus prompts the rememberer  
382 to recount presented events in order, starting with the beginning. This tendency is reflected in our  
383 findings’ second departure from typical free recall dynamics: a lack of increased probability of first  
384 recall for end-of-sequence events (Fig. 3A).

385 Thus, analyses such as those in Figure 3 that address only the temporal dynamics of free re-  
386 call paint an incomplete picture of memory for naturalistic episodes. While useful for studying  
387 presentation order-dependent recall dynamics, they neglect to consider the stimulus’s content (or,  
388 for example, that content’s potential interrelatedness). However, sensitivity to stimulus and recall  
389 content introduces a new challenge: distinguishing between levels of recall quality for a stimulus  
390 (i.e., an event) that is considered to have been “remembered.” When modeling memory experi-  
391 ments, often times events (or items) and their later memories are treated as binary and independent  
392 events (e.g., a given list item was simply either remembered or not remembered). Various models  
393 of memory (e.g., Yonelinas, 2002) attempt to improve upon this by including confidence ratings,  
394 rendering this binary judgement instead categorical. Our novel framework allows one to assess  
395 memory performance in a more continuous way (*precision*), as well as analyze the correlational  
396 structure of each encoding event to each memory event (*distinctiveness*). Further and importantly,  
397 these two novel metrics we introduce here arise from comparisons of the actual content of the  
398 experience/memories, which is not typically modeled. Leveraging this, we find that the successful  
399 memory performance is related to 1) the precision with which the participant recounts each event  
400 and 2) the distinctiveness of each recall event (relative to the other recalled events). The first finding  
401 suggests that the information retained for *any individual event* may predict the overall amount of  
402 information retained by the participant. The second finding suggests that the ability to distin-  
403 guish between temporally or semantically similar content is also related to the quantity of content  
404 recovered. Intriguingly, prior studies show that pattern separation, or the ability to discriminate  
405 between similar experiences, is impaired in many cognitive disorders as well as natural aging

406 (Stark et al., 2010; Yassa et al., 2011; Yassa and Stark, 2011). Future work might explore whether  
407 and how these metrics compare between cognitively impoverished groups and healthy controls.

408 While a large number of language models exist (e.g., WAS, LSA, word2vec, universal sentence  
409 encoder; Steyvers et al., 2004; Landauer et al., 1998; Mikolov et al., 2013; Cer et al., 2018), here  
410 we use latent dirichlet allocation (LDA)-based topic models for a few reasons. First, topic models  
411 capture the *essence* of a text passage devoid of the specific set and order of words used. This  
412 was an important feature of our model since different people may accurately recall a scene using  
413 very different language. Second, words can mean different things in different contexts (e.g. “bat”  
414 as the act of hitting a baseball, the object used for that action, or as a flying mammal). Topic  
415 models are robust to this, allowing words to exist as part of multiple topics. Last, topic models  
416 provide a straightforward means to recover the weights for the particular words comprising a topic,  
417 enabling easy interpretation of an event’s contents (e.g. Fig. 6). Other models such as Google’s  
418 universal sentence encoder offer a context-sensitive encoding of text passages, but the encoding  
419 space is complex and non-linear, and thus recovering the original words used to fit the model is  
420 not straightforward. However, it’s worth pointing out that our framework is divorced from the  
421 particular choice of language model. Moreover, many of the aspects of our framework could be  
422 swapped out for other choices. For example, the language model, the timeseries segmentation  
423 model and the video-recall matching function could all be customized for the particular problem.  
424 Indeed for some problems, recovery of the particular recall words may not be necessary, and thus  
425 other text-modeling approaches (such as universal sentence encoder) may be preferable. Future  
426 work will explore the influence of particular model choices on the framework’s accuracy.

427 Our work has broad implications for how we characterize and assess memory in real-world  
428 settings, such as the classroom or physician’s office. For example, the most commonly used  
429 classroom evaluation tools involve simply computing the proportion of correctly answered exam  
430 questions. Our work indicates that this approach is only loosely related to what educators might  
431 really want to measure: how well did the students understand the key ideas presented in the  
432 course? Under this typical framework of assessment, the same exam score of 50% could be  
433 ascribed to two very different students: one who attended the full course but struggled to learn

434 more than a broad overview of the material, and one who attended only half of the course but  
435 understood the material perfectly. Instead, one could apply our computational framework to build  
436 explicit content models of the course material and exam questions. This approach would provide  
437 a more nuanced and specific view into which aspects of the material students had learned well  
438 (or poorly). In clinical settings, memory measures that incorporate such explicit content models  
439 might also provide more direct evaluations of patients' memories.

440 **Methods**

441 **Experimental design and data collection**

442 Data were collected by Chen et al. (2017). In brief, participants ( $n = 17$ ) viewed the first 48 minutes  
443 of "A Study in Pink", the first episode of the BBC television series *Sherlock*, while fMRI volumes  
444 were collected (TR = 1500 ms). The stimulus was divided into a 23 min (946 TR) and a 25 min  
445 (1030 TR) segment to mitigate technical issues related to the scanner. After finishing the clip,  
446 participants were instructed to (quoting from Chen et al., 2017) "describe what they recalled of the  
447 [episode] in as much detail as they could, to try to recount events in the original order they were  
448 viewed in, and to speak for at least 10 minutes if possible but that longer was better. They were told  
449 that completeness and detail were more important than temporal order, and that if at any point  
450 they realized they had missed something, to return to it. Participants were then allowed to speak  
451 for as long as they wished, and verbally indicated when they were finished (e.g., 'I'm done')."  
452 For additional details about the experimental procedure and scanning parameters, see Chen et al.  
453 (2017). The experimental protocol was approved by Princeton University's Institutional Review  
454 Board.

455 After preprocessing the fMRI data and warping the images into a standard (3 mm<sup>3</sup> MNI) space,  
456 the voxel activations were z-scored (within voxel) and spatially smoothed using a 6 mm (full width  
457 at half maximum) Gaussian kernel. The fMRI data were also cropped so that all video-viewing  
458 data were aligned across participants. This included a constant 3 TR (4.5 s) shift to account for the

459 lag in the hemodynamic response. (All of these preprocessing steps followed Chen et al., 2017,  
460 where additional details may be found.)

461 **Data and code availability**

462 The fMRI data we analyzed are available online [here](#). The behavioral data and all of our analysis  
463 code may be downloaded [here](#).

464 **Statistics**

465 All statistical tests we performed were two-sided.

466 **Modeling the dynamic content of the video and recall transcripts**

467 **Topic modeling**

468 The input to the topic model we trained to characterize the dynamic content of the video comprised  
469 hand-generated annotations of each of 1000 scenes spanning the video clip (generated by Chen  
470 et al., 2017). The features annotated included: narrative details (a sentence or two describing  
471 what happened in that scene); whether the scene took place indoors or outdoors; names of any  
472 characters that appeared in the scene; name(s) of characters in camera focus; name(s) of characters  
473 who were speaking in the scene; the location (in the story) that the scene took place; camera angle  
474 (close up, medium, long, top, tracking, over the shoulder, etc.); whether music was playing in  
475 the scene or not; and a transcription of any on-screen text. We concatenated the text for all of  
476 these features within each segment, creating a “bag of words” describing each scene. We then  
477 re-organized the text descriptions into overlapping sliding windows spanning 50 scenes each.  
478 In other words, the first text sample comprised the combined text from the first 50 scenes (i.e.,  
479 1–50), the second comprised the text from scenes 2–51, and so on. We trained our model using  
480 these overlapping text samples with `scikit-learn` (version 0.19.1; Pedregosa et al., 2011), called  
481 from our high-dimensional visualization and text analysis software, `HyperTools` (Heusser et al.,  
482 2018b). Specifically, we used the `CountVectorizer` class to transform the text from each scene

483 into a vector of word counts (using the union of all words across all scenes as the “vocabulary,”  
484 excluding English stop words); this yielded a number-of-scenes by number-of-words *word count*  
485 matrix. We then used the `LatentDirichletAllocation` class (`topics=100, method='batch'`) to fit  
486 a topic model (Blei et al., 2003) to the word count matrix, yielding a number-of-scenes (1000) by  
487 number-of-topics (100) *topic proportions* matrix. The topic proportions matrix describes which mix  
488 of topics (latent themes) is present in each scene. Next, we transformed the topic proportions  
489 matrix to match the 1976 fMRI volume acquisition times. For each fMRI volume, we took the topic  
490 proportions from whatever scene was displayed for most of that volume’s 1500 ms acquisition time.  
491 This yielded a new number-of-TRs (1976) by number-of-topics (100) topic proportions matrix.

492 We created similar topic proportions matrices using hand-annotated transcripts of each partici-  
493 pant’s recall of the video (annotated by Chen et al., 2017). We tokenized the transcript into a list of  
494 sentences, and then re-organized the list into overlapping sliding windows spanning 10 sentences  
495 each; in turn we transformed each window’s sentences into a word count vector (using the same  
496 vocabulary as for the video model). We then used the topic model already trained on the video  
497 scenes to compute the most probable topic proportions for each sliding window. This yielded a  
498 number-of-sentences (range: 68–294) by number-of-topics (100) topic proportions matrix, for each  
499 participant. These reflected the dynamic content of each participant’s recalls. Note: for details  
500 on how we selected the video and recall window lengths and number of topics, see *Supporting*  
501 *Information* and Figure S1.

## 502 **Parsing topic trajectories into events using Hidden Markov Models**

503 We parsed the topic trajectories of the video and participants’ recalls into events using Hidden  
504 Markov Models (Rabiner, 1989). Given the topic proportions matrix (describing the mix of topics  
505 at each timepoint) and a number of states,  $K$ , an HMM recovers the set of state transitions that  
506 segments the timeseries into  $K$  discrete states. Following Baldassano et al. (2017), we imposed an  
507 additional set of constraints on the discovered state transitions that ensured that each state was  
508 encountered exactly once (i.e., never repeated). We used the BrainIAK toolbox (Capota et al., 2017)  
509 to implement this segmentation.

510 We used an optimization procedure to select the appropriate  $K$  for each topic proportions  
511 matrix. Specifically, we computed (for each matrix)

$$\operatorname{argmax}_K \left[ \frac{a}{b} - \frac{K}{\alpha} \right],$$

512 where  $a$  was the average correlation between the topic vectors of timepoints within the same state;  
513  $b$  was the average correlation between the topic vectors of timepoints within *different* states; and  
514  $\alpha$  was a regularization parameter that we set to 5 times the window length (i.e., 250 scenes for  
515 the video topic trajectory and 50 sentences for the recall topic trajectories). Figure 2B displays the  
516 event boundaries returned for the video, and Figure S4 displays the event boundaries returned  
517 for each participant's recalls. After obtaining these event boundaries, we created stable estimates  
518 of each topic proportions matrix by averaging the topic vectors within each event. This yielded a  
519 number-of-events by number-of-topics matrix for the video and recalls from each participant.

520 We also evaluated a parameter-free procedure for choosing  $K$ , which finds the  $K$  value that  
521 maximizes the Wasserstein distance (a.k.a. "Earth mover's" distance) between the within and  
522 across event distributions of correlation values. This alternative procedure largely replicated the  
523 pattern of results found with the parameterized method described above, but recovered sub-  
524 stantially fewer events on average (Fig.S6). While both approaches seem to underestimate the  
525 number of video/recall events relative to the "true" number (as determined by human raters), the  
526 parameterized approach was closer to the true number.

527 **Naturalistic extensions of classic list-learning analyses**

528 In traditional list-learning experiments, participants view a list of items (e.g., words) and then recall  
529 the items later. Our video-recall event matching approach affords us the ability to analyze memory  
530 in a similar way. The video and recall events can be treated analogously to studied and recalled  
531 "items" in a list-learning study. We can then extend classic analyses of memory performance and  
532 dynamics (originally designed for list-learning experiments) to the more naturalistic video recall  
533 task used in this study.

534 Perhaps the simplest and most widely used measure of memory performance is *accuracy*—i.e.,  
535 the proportion of studied (experienced) items (in this case, the 34 video events) that the participant  
536 later remembered. Chen et al. (2017) developed a human rating system whereby the quality of  
537 each participant’s memory was evaluated by an independent rater. We found a strong across-  
538 participants correlation between these independant ratings and the overall number of events that  
539 our HMM approach identified in participants’ recalls (Pearson’s  $r(15) = 0.67, p = 0.003$ ).

540 As described below, we next considered a number of memory performance measures that are  
541 typically associated with list-learning studies. We also provide a software package, Quail, for  
542 carrying out these analyses (Heusser et al., 2017).

543 **Probability of first recall (PFR).** PFR curves (Welch and Burnett, 1924; Postman and Phillips,  
544 1965; Atkinson and Shiffrin, 1968) reflect the probability that an item will be recalled first as a  
545 function of its serial position during encoding. To carry out this analysis, we initialized a number-  
546 of-participants (17) by number-of-video-events (34) matrix of zeros. Then for each participant, we  
547 found the index of the video event that was recalled first (i.e., the video event whose topic vector  
548 was most strongly correlated with that of the first recall event) and filled in that index in the matrix  
549 with a 1. Finally, we averaged over the rows of the matrix, resulting in a 1 by 34 array representing  
550 the proportion of participants that recalled an event first, as a function of the order of the event’s  
551 appearance in the video (Fig. 3A).

552 **Lag conditional probability curve (lag-CRP).** The lag-CRP curve (Kahana, 1996) reflects the  
553 probability of recalling a given event after the just-recalled event, as a function of their relative  
554 positions (or *lag*). In other words, a lag of 1 indicates that a recalled event came immediately after  
555 the previously recalled event in the video, and a lag of -3 indicates that a recalled event came 3  
556 events before the previously recalled event. For each recall transition (following the first recall),  
557 we computed the lag between the current recall event and the next recall event, normalizing by  
558 the total number of possible transitions. This yielded a number-of-participants (17) by number-  
559 of-lags (-33 to +33; 67 lags total) matrix. We averaged over the rows of this matrix to obtain a

560 group-averaged lag-CRP curve (Fig. 3B).

561 **Serial position curve (SPC).** SPCs (Murdock, 1962) reflect the proportion of participants that  
562 remember each item as a function of the items' serial position during encoding. We initialized  
563 a number-of-participants (17) by number-of-video-events (34) matrix of zeros. Then, for each  
564 recalled event, for each participant, we found the index of the video event that the recalled event  
565 most closely matched (via the correlation between the events' topic vectors) and entered a 1 into  
566 that position in the matrix (i.e., for the given participant and event). This resulted in a matrix  
567 whose entries indicated whether or not each event was recalled by each participant (depending  
568 on whether the corresponding entires were set to one or zero). Finally, we averaged over the rows  
569 of the matrix to yield a 1 by 34 array representing the proportion of participants that recalled each  
570 event as a function of the order of the event's appearance in the video (Fig. 3C).

571 **Temporal clustering scores.** Temporal clustering describes participants' tendency to organize  
572 their recall sequences by the learned items' encoding positions. For instance, if a participant  
573 recalled the video events in the exact order they occurred (or in exact reverse order), this would  
574 yield a score of 1. If a participant recalled the events in random order, this would yield an expected  
575 score of 0.5. For each recall event transition (and separately for each participant), we sorted  
576 all not-yet-recalled events according to their absolute lag (i.e., distance away in the video). We  
577 then computed the percentile rank of the next event the participant recalled. We averaged these  
578 percentile ranks across all of the participant's recalls to obtain a single temporal clustering score  
579 for the participant.

580 **Semantic clustering scores.** Semantic clustering describes participants' tendency to recall seman-  
581 tically similar presented items together in their recall sequences. Here, we used the topic vectors  
582 for each event as a proxy for its semantic content. Thus, the similarity between the semantic  
583 content for two events can be computed by correlating their respective topic vectors. For each  
584 recall event transition, we sorted all not-yet-recalled events according to how correlated the topic  
585 vector of the closest-matching video event was to the topic vector of the closest-matching video event

586 to the just-recalled event. We then computed the percentile rank of the observed next recall. We  
587 averaged these percentile ranks across all of the participant's recalls to obtain a single semantic  
588 clustering score for the participant.

589 **Novel naturalistic memory metrics**

590 **Precision.** We tested whether participants who recalled more events were also more *precise* in their  
591 recollections. For each participant, we computed the correlation between the topic vectors for each  
592 recall event and that of its closest-matching video event (only for the events which they recalled).  
593 We Fisher's *z*-transformed the correlations, computed the average and then inverse Fisher's *z*-  
594 transformed the resulting value. This gave a single value per participant representing the average  
595 precision across all recalled events. We then correlated this value with hand-annotated as well as  
596 model derived (e.g.  $k$  or the number of events recovered by the HMM) memory performance.

597 **Distinctiveness.** We also considered the *distinctiveness* of each recalled event. That is, how  
598 uniquely a recalled event's topic vector matched a given video event topic vector, versus the  
599 topic vectors for the other video events. We hypothesized that participants with high memory  
600 performance might describe each event in a more distinctive way (relative to those with lower  
601 memory performance who might describe events in a more general way). To test this hypothesis  
602 we define a distinctiveness score for each recalled event as

$$d(\text{event}) = 1 - \bar{c}(\text{event}),$$

603 where  $\bar{c}(\text{event})$  is the average correlation between the given recalled event's topic vector and the  
604 topic vectors from all video events *except* the best-matching video event. We then averaged these  
605 distinctiveness scores across all of the events recalled by the given participant. As above, we used  
606 Fisher's *z*-transform (and inverse-transform) before/after averaging correlation values. Finally,  
607 we correlated these values with hand-annotated and model derived memory performance scores  
608 across-subjects.

609 **Visualizing the video and recall topic trajectories**

610 We used the UMAP algorithm (McInnes and Healy, 2018) to project the 100-dimensional topic space  
611 onto a two-dimensional space for visualization (Figs. 5, 6). To ensure that all of the trajectories were  
612 projected onto the *same* lower dimensional space, we computed the low-dimensional embedding  
613 on a “stacked” matrix created by vertically concatenating the events-by-topics topic proportions  
614 matrices for the video and all 17 participants’ recalls. We then divided the rows of the result (a  
615 total-number-of-events by two matrix) back into separate matrices for the video topic trajectory  
616 and the trajectories for each participant’s recalls (Fig. 5). This general approach for discovering  
617 a shared low-dimensional embedding for a collections of high-dimensional observations follows  
618 Heusser et al. (2018b).

619 **Estimating the consistency of flow through topic space across participants**

620 In Figure 5B, we present an analysis aimed at characterizing locations in topic space that dif-  
621 ferent participants move through in a consistent way (via their recall topic trajectories). The  
622 two-dimensional topic space used in our visualizations (Fig. 5) ranged from -5 to 5 (arbitrary) units  
623 in the  $x$  dimension and from -6.5 to 2 units in the  $y$  dimension. We divided this space into a grid  
624 of vertices spaced 0.25 units apart. For each vertex, we examined the set of line segments formed  
625 by connecting each pair successively recalled events, across all participants, that passed within 0.5  
626 units. We computed the distribution of angles formed by those segments and the  $x$ -axis, and used a  
627 Rayleigh test to determine whether the distribution of angles was reliably “peaked” (i.e., consistent  
628 across all transitions that passed through that local portion of topic space). To create Figure 5B we  
629 drew an arrow originating from each grid vertex, pointing in the direction of the average angle  
630 formed by line segments that passed within 0.5 units. We set the arrow lengths to be inversely  
631 proportional to the  $p$ -values of the Rayleigh tests at each vertex. Specifically, for each vertex we  
632 converted all of the angles of segments that passed within 0.5 units to unit vectors, and we set  
633 the arrow lengths at each vertex proportional to the length of the (circular) mean vector. We also  
634 indicated any significant results ( $p < 0.05$ , corrected using the Benjamani-Hochberg procedure) by

635 coloring the arrows in blue (darker blue denotes a lower  $p$ -value, i.e., a longer mean vector); all  
636 tests with  $p \geq 0.05$  are displayed in gray and given a lower opacity value.

637 **Searchlight fMRI analyses**

638 In Figure 7, we present two analyses aimed at identifying brain structures whose responses (as  
639 participants viewed the video) exhibited particular temporal correlations. We developed a search-  
640 light analysis whereby we constructed a cube centered on each voxel (radius: 5 voxels). For each  
641 of these cubes, we computed the temporal correlation matrix of the voxel responses during video  
642 viewing. Specifically, for each of the 1976 volumes collected during video viewing, we correlated  
643 the activity patterns in the given cube with the activity patterns (in the same cube) collected during  
644 every other timepoint. This yielded a 1976 by 1976 correlation matrix for each cube.

645 Next, we constructed two sets of “template” matrices: one reflecting the video’s topic trajectory  
646 and the other reflecting each participant’s recall topic trajectory. To construct the video template, we  
647 computed the correlations between the topic proportions estimated for every pair of TRs (prior to  
648 segmenting the trajectory into discrete events; i.e., the correlation matrix shown in Figs. 2B and 7A).  
649 We constructed similar temporal correlation matrices for each participant’s recall topic trajectory  
650 (Figs. 2D, S4). However, to correct for length differences and potential non-linear transformations  
651 between viewing time and recall time, we first used dynamic time warping (Berndt and Clifford,  
652 1994) to temporally align participants’ recall topic trajectories with the video topic trajectory (an  
653 example correlation matrix before and after warping is shown in Fig. 7B). This yielded a 1976 by  
654 1976 correlation matrix for the video template and for each participant’s recall template.

655 To determine which (cubes of) voxel responses reliably matched the video template, we cor-  
656 related the upper triangle of the voxel correlation matrix for each cube with the upper triangle  
657 of the video template matrix (Kriegeskorte et al., 2008). This yielded, for each participant, a  
658 single correlation value. We computed the average (Fisher  $z$ -transformed) correlation coefficient  
659 across participants. We used a permutation-based procedure to assess significance, whereby we  
660 re-computed the average correlations for each of 100 “null” video templates (constructed by circu-  
661 larly shifting the template by a random number of timepoints). (For each permutation, the same

shift was used for all participants.) We then estimated a  $p$ -value by computing the proportion of shifted correlations that were larger than the observed (unshifted) correlation. To create the map in Figure 7A we thresholded out any voxels whose correlation values fell below the 95<sup>th</sup> percentile of the permutation-derived null distribution.

We used a similar procedure to identify which voxels' responses reflected the recall templates. For each participant, we correlated the upper triangle of the correlation matrix for each cube of voxels with their (time warped) recall correlation matrix. As in the video template analysis this yielded a single correlation coefficient for each participant. However, whereas the video analysis compared every participant's responses to the same template, here the recall templates were unique for each participant. We computed the average z-transformed correlation coefficient across participants, and used the same permutation procedure we developed for the video responses to assess significant correlations. To create the map in Figure 7B we thresholded out any voxels whose correlation values fell below the 95<sup>th</sup> percentile of the permutation-derived null distribution.

## References

- Atkinson, R. C. and Shiffrin, R. M. (1968). Human memory: A proposed system and its control processes. In Spence, K. W. and Spence, J. T., editors, *The psychology of learning and motivation*, volume 2, pages 89–105. Academic Press, New York.
- Baldassano, C., Chen, J., Zadbood, A., Pillow, J. W., Hasson, U., and Norman, K. A. (2017). Discovering event structure in continuous narrative perception and memory. *Neuron*, 95(3):709–721.
- Berndt, D. J. and Clifford, J. (1994). Using dynamic time warping to find patterns in time series. In *KDD workshop*, volume 10, pages 359–370.
- Blei, D. M. and Lafferty, J. D. (2006). Dynamic topic models. In *Proceedings of the 23rd International Conference on Machine Learning*, ICML '06, pages 113–120, New York, NY, US. ACM.

- 686 Blei, D. M., Ng, A. Y., and Jordan, M. I. (2003). Latent dirichlet allocation. *Journal of Machine*  
687 *Learning Research*, 3:993 – 1022.
- 688 Brunec, I. K., Moscovitch, M. M., and Barense, M. D. (2018). Boundaries shape cognitive represen-  
689 tations of spaces and events. *Trends in Cognitive Sciences*, 22(7):637–650.
- 690 Bylinskii, Z., Isola, P., Bainbridge, C., Torralba, A., and Oliva, A. (2015). Intrinsic and extrinsic  
691 effects on image memorability. *Vision Research*, 116:165–178.
- 692 Capota, M., Turek, J., Chen, P.-H., Zhu, X., Manning, J. R., Sundaram, N., Keller, B., Wang, Y., and  
693 Shin, Y. S. (2017). Brain imaging analysis kit.
- 694 Cer, D., Yang, Y., y Kong, S., Hua, N., Limtiaco, N., John, R. S., Constant, N., Guajardo-Cespedes,  
695 M., Yuan, S., Tar, C., Sung, Y.-H., Strope, B., and Kurzweil, R. (2018). Universal sentence encoder.  
696 *arXiv*, 1803.11175.
- 697 Chen, J., Leong, Y. C., Honey, C. J., Yong, C. H., Norman, K. A., and Hasson, U. (2017). Shared  
698 memories reveal shared structure in neural activity across individuals. *Nature Neuroscience*,  
699 20(1):115.
- 700 Chun, M. and Turk-Browne, N. (2007). Interactions between attention and memory. *Current opinion*  
701 *in neurobiology*, 17(2):177–184.
- 702 Clewett, D. and Davachi, L. (2017). The ebb and flow of experience determines the temporal  
703 structure of memory. *Curr Opin Behav Sci*, 17:186–193.
- 704 Davachi, L. (2006). Item, context and relational episodic encoding in humans. *Current Opinion in*  
705 *Neurobiology*, 16(6):693—700.
- 706 Davachi, L., Mitchell, J. P., and Wagner, A. D. (2003). Multiple routes to memory: distinct medial  
707 temporal lobe processes build item and source memories. *Proceedings of the National Academy of*  
708 *Sciences, USA*, 100(4):2157 – 2162.

- 709 Diana, R. A., Yonelinas, A. P., and Ranganath, C. (2007). Imaging recollection and famil-  
710 iarity in the medial temporal lobe: a three-component model. *Trends in Cognitive Sciences*,  
711 doi:10.1016/j.tics.2007.08.001.
- 712 DuBrow, S. and Davachi, L. (2013). The influence of contextual boundaries on memory for the  
713 sequential order of events. *Journal of Experimental Psychology: General*, 142(4):1277–1286.
- 714 Ezzyat, Y. and Davachi, L. (2011). What constitutes an episode in episodic memory? *Psychological  
715 Science*, 22(2):243–252.
- 716 Friendly, M., Franklin, P. E., Hoffman, D., and Rubin, D. C. (1982). The Toronto Word Pool:  
717 Norms for imagery, concreteness, orthographic variables, and grammatical usage for 1,080  
718 words. *Behavior Research Methods and Instrumentation*, 14:375–399.
- 719 Gilboa, A. and Marlatte, H. (2017). Neurobiology of schemas and schema-mediated memory.  
720 *Trends Cogn Sci*, 21(8):618–631.
- 721 Heusser, A. C., Ezzyat, Y., Shiff, I., and Davachi, L. (2018a). Perceptual boundaries cause mnemonic  
722 trade-offs between local boundary processing and across-trial associative binding. *Journal of  
723 Experimental Psychology Learning, Memory, and Cognition*, 44(7):1075–1090.
- 724 Heusser, A. C., Fitzpatrick, P. C., Field, C. E., Ziman, K., and Manning, J. R. (2017). Quail: a  
725 Python toolbox for analyzing and plotting free recall data. *The Journal of Open Source Software*,  
726 10.21105/joss.00424.
- 727 Heusser, A. C., Ziman, K., Owen, L. L. W., and Manning, J. R. (2018b). HyperTools: a Python  
728 toolbox for gaining geometric insights into high-dimensional data. *Journal of Machine Learning  
729 Research*, 18(152):1–6.
- 730 Howard, M. W. and Kahana, M. J. (2002). A distributed representation of temporal context. *Journal  
731 of Mathematical Psychology*, 46:269–299.
- 732 Howard, M. W., MacDonald, C. J., Tiganj, Z., Shankar, K. H., Du, Q., Hasselmo, M. E., and H., E.

- 733 (2014). A unified mathematical framework for coding time, space, and sequences in the medial  
734 temporal lobe. *Journal of Neuroscience*, 34(13):4692–4707.
- 735 Howard, M. W., Viskontas, I. V., Shankar, K. H., and Fried, I. (2012). Ensembles of human MTL  
736 neurons “jump back in time” in response to a repeated stimulus. *Hippocampus*, 22:1833–1847.
- 737 Huk, A., Bonnen, K., and He, B. J. (2018). Beyond trial-based paradigms: continuous behavior, on-  
738 going neural activity, and naturalistic stimuli. *Journal of Neuroscience*, 10.1523/JNEUROSCI.1920-  
739 17.2018.
- 740 Kahana, M. J. (1996). Associative retrieval processes in free recall. *Memory & Cognition*, 24:103–109.
- 741 Koriat, A. and Goldsmith, M. (1994). Memory in naturalistic and laboratory contexts: distin-  
742 guishing accuracy-oriented and quantity-oriented approaches to memory assessment. *Journal of*  
743 *Experimental Psychology: General*, 123(3):297–315.
- 744 Kriegeskorte, N., Mur, M., and Bandettini, P. (2008). Representational similarity analysis – con-  
745 nnecting the branches of systems neuroscience. *Frontiers in Systems Neuroscience*, 2:1 – 28.
- 746 Landauer, T. K., Foltz, P. W., and Laham, D. (1998). Introduction to latent semantic analysis.  
747 *Discourse Processes*, 25:259–284.
- 748 Lerner, Y., Honey, C. J., Silbert, L. J., and Hasson, U. (2011). Topographic mapping of a hierarchy  
749 of temporal receptive windows using a narrated story. *Journal of Neuroscience*, 31(8):2906–2915.
- 750 Manning, J. R. (2019). Episodic memory: mental time travel or a quantum ‘memory wave’ function?  
751 *PsyArXiv*, doi:10.31234/osf.io/6zjwb.
- 752 Manning, J. R., Norman, K. A., and Kahana, M. J. (2015). The role of context in episodic memory.  
753 In Gazzaniga, M., editor, *The Cognitive Neurosciences, Fifth edition*, pages 557–566. MIT Press.
- 754 Manning, J. R., Polyn, S. M., Baltuch, G., Litt, B., and Kahana, M. J. (2011). Oscillatory patterns  
755 in temporal lobe reveal context reinstatement during memory search. *Proceedings of the National*  
756 *Academy of Sciences, USA*, 108(31):12893–12897.

- 757 McInnes, L. and Healy, J. (2018). UMAP: Uniform manifold approximation and projection for  
758 dimension reduction. *arXiv*, 1802(03426).
- 759 Mikolov, T., Chen, K., Corrado, G., and Dean, J. (2013). Efficient estimation of word representations  
760 in vector space. *arXiv*, 1301.3781.
- 761 Mueller, A., Fillion-Robin, J.-C., Boidol, R., Tian, F., Nechifor, P., yoonsubKim, Peter, Rampin, R.,  
762 Corvellec, M., Medina, J., Dai, Y., Petrushev, B., Langner, K. M., Hong, Alessio, Ozsvald, I.,  
763 vkolmakov, Jones, T., Bailey, E., Rho, V., IgorAPM, Roy, D., May, C., foobuzz, Piyush, Seong,  
764 L. K., Goey, J. V., Smith, J. S., Gus, and Mai, F. (2018). WordCloud 1.5.0: a little word cloud  
765 generator in Python. *Zenodo*, <https://zenodo.org/record/1322068#.W4tPKZNKh24>.
- 766 Murdock, B. B. (1962). The serial position effect of free recall. *Journal of Experimental Psychology*,  
767 64:482–488.
- 768 Paller, K. A. and Wagner, A. D. (2002). Observing the transformation of experience into memory.  
769 *Trends in Cognitive Sciences*, 6(2):93–102.
- 770 Pedregosa, F., Varoquaux, G., Gramfort, A., Michel, V., Thirion, B., Grisel, O., Blondel, M., Pretten-  
771 hofer, P., Weiss, R., Dubourg, V., Vanderplas, J., Passos, A., Cournapeau, D., Brucher, M., Perrot,  
772 M., and Duchesnay, E. (2011). Scikit-learn: Machine learning in Python. *Journal of Machine  
773 Learning Research*, 12:2825–2830.
- 774 Polyn, S. M., Norman, K. A., and Kahana, M. J. (2009). A context maintenance and retrieval model  
775 of organizational processes in free recall. *Psychological Review*, 116(1):129–156.
- 776 Postman, L. and Phillips, L. W. (1965). Short-term temporal changes in free recall. *Quarterly Journal  
777 of Experimental Psychology*, 17:132–138.
- 778 Rabiner, L. (1989). A tutorial on Hidden Markov Models and selected applications in speech  
779 recognition. *Proceedings of the IEEE*, 77(2):257–286.
- 780 Radvansky, G. A. and Zacks, J. M. (2017). Event boundaries in memory and cognition. *Curr Opin  
781 Behav Sci*, 17:133–140.

- 782 Ranganath, C., Cohen, M. X., Dam, C., and D'Esposito, M. (2004). Inferior temporal, prefrontal,  
783 and hippocampal contributions to visual working memory maintenance and associative memory  
784 retrieval. *Journal of Neuroscience*, 24(16):3917–3925.
- 785 Ranganath, C. and Ritchey, M. (2012). Two cortical systems for memory-guided behavior. *Nature  
786 Reviews Neuroscience*, 13:713 – 726.
- 787 Schlichting, M. L. and Preston, A. R. (2015). Memory integration: neural mechanisms and impli-  
788 cations for behavior. *Current Opinion in Behavioral Sciences*, 1:1–8.
- 789 Simony, E., Honey, C. J., Chen, J., and Hasson, U. (2016). Uncovering stimulus-locked network  
790 dynamics during narrative comprehension. *Nature Communications*, 7(12141):1–13.
- 791 Spalding, K. N., Schlichting, M. L., Zeithamova, D., Preston, A. R., Tranel, D., Duff, M. C., and  
792 Warren, D. E. (2018). Ventromedial prefrontal cortex is necessary for normal associative inference  
793 and memory integration. *The Journal of Neuroscience*, 38(15):3767–3775.
- 794 Stark, S. M., Yassa, M. A., and Stark, C. E. L. (2010). Individual differences in spatial pattern  
795 separation performance associated with healthy aging in humans. *Learning & Memory*, 17(6):284–  
796 288.
- 797 Steyvers, M., Shiffrin, R. M., and Nelson, D. L. (2004). Word association spaces for predicting  
798 semantic similarity effects in episodic memory. In Healy, A. F., editor, *Cognitive Psychology and  
799 its Applications: Festschrift in Honor of Lyle Bourne, Walter Kintsch, and Thomas Landauer*. American  
800 Psychological Association, Washington, DC.
- 801 Tompry, A. and Davachi, L. (2017). Consolidation promotes the emergence of representational  
802 overlap in the hippocampus and medial prefrontal cortex. *Neuron*, 96(1):228–241.
- 803 Tyng, C. M., Amin, H. U., Saad, M. N. M., and S, M. A. (2017). The influences of emotion on  
804 learning and memory. *Frontiers in psychology*, 8:1454.
- 805 van Kesteren, M. T. R., Beul, S. F., Takashima, A., Henson, R. N., Ruiter, D. J., and Fernández, G.

- 806 (2013). Differential roles for medial prefrontal and medial temporal cortices in schema-dependent  
807 encoding: from congruent to incongruent. *Neuropsychologia*, 51(12):2352–2359.
- 808 van Kesteren, M. T. R., Ruiter, D. J., Fernández, G., and Henson, R. N. (2012). How schema and  
809 novelty augment memory formation. *Trends Neurosci*, 35(4):211–9.
- 810 Waskom, M., Botvinnik, O., Okane, D., Hobson, P., David, Halchenko, Y., Lukauskas, S., Cole, J. B.,  
811 Warmenhoven, J., de Ruiter, J., Hoyer, S., Vanderplas, J., Villalba, S., Kunter, G., Quintero, E.,  
812 Martin, M., Miles, A., Meyer, K., Augspurger, T., Yarkoni, T., Bachant, P., Williams, M., Evans,  
813 C., Fitzgerald, C., Brian, Wehner, D., Hitz, G., Ziegler, E., Qalieh, A., and Lee, A. (2016). Seaborn:  
814 v0.7.1.
- 815 Welch, G. B. and Burnett, C. T. (1924). Is primacy a factor in association-formation. *American Journal  
816 of Psychology*, 35:396–401.
- 817 Wiltgen, B. J. and Silva, A. J. (2007). Memory for context becomes less specific with time. *Learning  
818 & Memory*, 14(4):313–317.
- 819 Yassa, M. A., Lacy, J. W., Stark, S. M., Albert, M. S., Gallagher, M., and Stark, C. E. L. (2011). Pattern  
820 separation deficits associated with increased hippocampal ca3 and dentate gyrus activity in  
821 nondemented older adults. *Hippocampus*, 21(9):968–979.
- 822 Yassa, M. A. and Stark, C. E. L. (2011). Pattern separation in the hippocampus. *Trends In Neuro-  
823 sciences*, 34(10):515–525.
- 824 Yonelinas, A. P. (2002). The nature of recollection and familiarity: A review of 30 years of research.  
825 *Journal of Memory and Language*, 46:441–517.
- 826 Zacks, J. M., Speer, N. K., Swallow, K. M., Braver, T. S., and Reynolds, J. R. (2007). Event perception:  
827 a mind-brain perspective. *Psychological Bulletin*, 133:273–293.
- 828 Zadbood, A., Chen, J., Leong, Y. C., Norman, K. A., and Hasson, U. (2017). How we transmit  
829 memories to other brains: Constructing shared neural representations via communication. *Cereb  
830 Cortex*, 27(10):4988–5000.

831 Zwaan, R. A. and Radvansky, G. A. (1998). Situation models in language comprehension and  
832 memory. *Psychological Bulletin*, 123(2):162 – 185.

## 833 **Supporting information**

834 Supporting information is available in the online version of the paper.

## 835 **Acknowledgements**

836 We thank Luke Chang, Janice Chen, Chris Honey, Lucy Owen, Emily Whitaker, and Kirsten Ziman  
837 for feedback and scientific discussions. We also thank Janice Chen, Yuan Chang Leong, Kenneth  
838 Norman, and Uri Hasson for sharing the data used in our study. Our work was supported in part  
839 by NSF EPSCoR Award Number 1632738. The content is solely the responsibility of the authors  
840 and does not necessarily represent the official views of our supporting organizations.

## 841 **Author contributions**

842 Conceptualization: A.C.H. and J.R.M.; Methodology: A.C.H. and J.R.M.; Software: A.C.H., P.C.F.  
843 and J.R.M.; Analysis: A.C.H., P.C.F. and J.R.M.; Writing, Reviewing, and Editing: A.C.H., P.C.F.  
844 and J.R.M.; Supervision: J.R.M.

## 845 **Author information**

846 The authors declare no competing financial interests. Correspondence and requests for materials  
847 should be addressed to J.R.M. (jeremy.r.manning@dartmouth.edu).